Sampling technique for achieving full unit-circle coverage using a real-axis spatial light modulator

Steve Serati and Kipp Bauchert
Boulder Nonlinear Systems, Inc.
450 Courtney Way, #107
Lafeyette, Colorado 80026

ABSTRACT

We investigate the possibility of using a real-axis spatial light modulator (SLM) to realize complex-amplitude modulation with full coverage over the unit circle. The real-axis SLM produces a pixelated bipolar-amplitude wavefront. Each pixel is basically a spatial pulse width with the signal information being carried by the pulse's amplitude. Data streams generated in this manner have real and imaginary components due to the relative even and odd symmetry of the pulse amplitude modulation. When the pulse rate is twice the minimum Nyquist rate for band-limited amplitude modulation, it is possible to resolve the signal into its quadrature phase components (real and imaginary terms). By changing the relative amplitude of these quadrature phase terms, any value within the complex plane is accessible. Since the SLM does not have any optical gain, coverage is limited to the unit circle in the complex plane.

Keywords: Complex-amplitude, real-axis spatial light modulator, optical processing

1. INTRODUCTION

A signal, which is composed of even and odd components, requires complex values to fully define its content. Complex-valued functions are represented by linear combinations of real and imaginary values, which may reside anywhere in the complex plane. However, practical optical processors use optically passive elements, which restrict the complex values to the unit circle as shown in Figure 1.

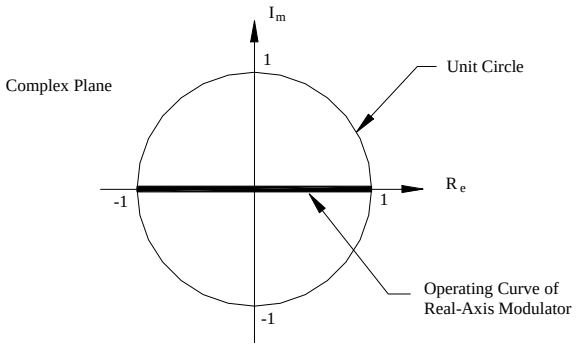

Figure 1. Real-axis modulation in relation to the complex unit circle.

A spatial light modulator (SLM) which provides full coverage of the unit circle is important, because it places fewer constraints on the processing algorithm, which extracts information from the signal[1]. Because

of its importance, a variety of methods for achieving full unit-circle coverage have been investigated. These methods include, but are not limited to, offsetting sample locations,[2,3,4] under-resolving macropixels,[5,6] pseudorandom encoding[7] and combining outputs from two SLMs[8]. The technique presented in this paper is similar in nature to the first two approaches mentioned. However, this one is based on using an analog ferroelectric liquid crystal (FLC) modulator to achieve an on-axis Fourier transform response. In this approach, the FLC modulator provides bipolar-amplitude (real-axis) modulation as shown in Figure 1. In the other approaches, the light modulators are either unipolar-amplitude or optical path difference (OPD) components, which are implemented with amplitude masks, phase masks, nematic liquid crystal displays or deformable mirror displays.

A ferroelectric real-axis modulator, as implemented on a VLSI backplane, has a channel capacity that exceeds 40,000 bits/second. This is the information-transmission rate per pixel based on the bandwidth and contrast ratio of the FLC modulator[9]. With this channel capacity, a 512 x 512 SLM is capable of loading over 10 Gigabits per second into an optical processor. Of course, this potential is difficult to realize using today's drive schemes, but much of this potential is accessible through better electronics. In addition to the processing potential, the analog FLC modulator offers an economical means for obtaining complex modulation. With real-axis modulation, only two pixels are needed to define any point in the unit circle as compared with unipolar modulators where three or more pixels are needed[4]. The modulator uses voltage levels that make it well suited for VLSI backplanes. This not only makes high-speed backplanes more manufacturable, but it also allows for high-resolution designs. Also, the real-axis modulator is easier to fabricate than most of its cousins including the bistable modulator. For these reasons, complex-amplitude modulation using a real-axis modulator is investigated in this paper.

2. METHOD

One technique for converting amplitude-only modulation into complex modulation is to use a detour phase (delayed sampling) technique which was first demonstrated by Brown and Lohmann[2]. Their binary technique used the relative position and size of transparent boxes to realize complex spatial filters. This basic technique has been proven to work with a variety of amplitude and limited-phase modulators.[3,10,11] The extension of this technique to real-axis modulation is straightforward. While real-axis modulation reduces the number of pixels per complex data point (two pixels instead of three or four), it does not significantly change the procedure. Unfortunately, the image and its conjugate occur as diffracted orders even with a real-axis modulator. This means that the image information resides on a carrier frequency, which prevents using this technique for generating on-axis complex spatial filters. Therefore, this paper introduces a different approach, which generates the phase relationships needed for on-axis operation.

In this approach, we use the fact that the real-axis modulator produces only real-valued functions. These functions (i.e. images or filters) are composed of even and odd terms. That is

$$f(x) = f_e(x) + f_o(x) \ , \tag{1}$$

where the even, $f_e(x)$, and odd, $f_o(x)$, terms are also real functions. The Fourier transform of $f(x)$ is Hermitian, which is the summation of a real-even and an imaginary-odd function. To examine the relationship between the real and imaginary components of the transform, we write $f(x)$ as a Fourier series and ignore the effects produced by the SLM backplane. These effects enter the discussion later. As a Fourier series, $f(x)$ is written as

$$f(x) = a_o + \sum_{n=1}^{\infty} (a_n \cos n\omega_o x + b_n \sin n\omega_o x) \ , \tag{2}$$

where $n\omega_o$ represents the discreet frequencies of the Fourier series and the corresponding coefficients are:

$$a_o = F_o = \frac{2}{(x_2 - x_1)} \int_{x_1}^{x_2} f(x)dx,$$

$$a_n = [F_n + F_{-n}] = 2\,\mathrm{Re}\{F_n\} = \frac{2}{(x_2 - x_1)} \int_{x_1}^{x_2} f(x)\cos n\omega_o x dx,$$

$$b_n = j[F_n - F_{-n}] = -2\,\mathrm{Im}\{F_n\} = \frac{2}{(x_2 - x_1)} \int_{x_1}^{x_2} f(x)\sin n\omega_o x dx,$$

$$F_n = \frac{1}{2}(a_n - jb_n).$$

As defined, the a_n and b_n values represent the real-even and imaginary-odd terms of the series, respectively. By using Euler's indentities and rearranging terms, we have

$$f(x) = a_o + \frac{1}{2}\sum_{n=1}^{\infty}(a_n - jb_n)e^{jn\omega_o x} + (a_n + jb_n)e^{-jn\omega_o x}, \quad (3)$$

or

$$f(x) = a_o + \frac{1}{2}\sum_{n=1}^{\infty}(a_n - b_n e^{j\pi/2})e^{jn\omega_o x} + (a_n + b_n e^{j\pi/2})e^{-jn\omega_o x}. \quad (4)$$

From Equations 3 and 4, it can be seen that the a_n and b_n terms are quadrature phasors that rotate at the rate of $n\omega_o$. These phasors combine to represent one unique point, c_n, in the unit circle as follows:

$$c_n = \sqrt{a_n^2 + b_n^2}, \quad (5)$$

$$\phi_n = \tan^{-1}(-b_n / a_n). \quad (6)$$

By varying the amplitude of a_n and b_n between –1 and 1, any point in the unit circle is represented. Unfortunately, these in-phase and quadrature phasors are only mathematical representations of the complex Fourier components and not physically realizable without a complex modulator. However, the Fourier components are defined by any set of two or more phasors that are not collinear. Therefore, we can use a different set of phasors, which have amplitudes of p_k and p_l and are phase shifted by $\pm\pi/4$, to represent the a_n and b_n terms as shown in Figure 2.

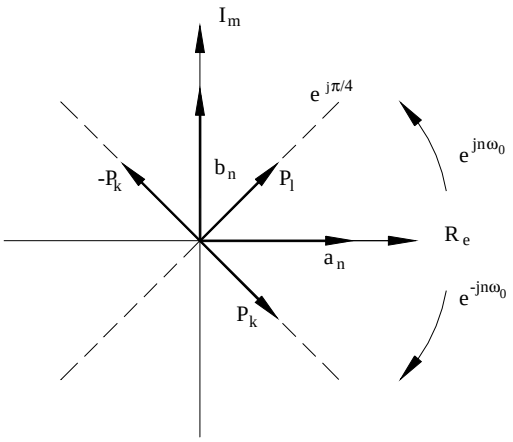

Figure 2. Phasor diagram for sampling technique.

The phasor diagram of Figure 2 is mathematically represented as:

$$a_n = p_k e^{-j\pi/4} + p_l e^{j\pi/4}, \tag{7}$$

$$-b_n e^{j\pi/2} = p_k e^{-j\pi/4} - p_l e^{j\pi/4}. \tag{8}$$

As with the detour phase technique discussed above, it is possible to produce a phase shift by changing the position of the sample location. However, our on-axis approach adds some complexity. If we simply offset the sample location with respect to the normal location of the $n\omega_o$ terms in the Fourier domain, then we have misaligned the filter. As shown by Equation 9, a frequency shift arises from the frequency-translation property, where a change of position in the Fourier domain is equivalent to the spatial-domain operation of multiplying the function by a linear phase. However, this spatial-domain operation in an optical correlator represents an input image that is tilted off axis with respect to the filter plane.

$$e^{j\omega_o x} f(x) \leftrightarrow F(\omega - \omega_o) \tag{9}$$

Instead of shifting the sample locations, the approach here is to oversample the Fourier plane. However, this requires the energy in the Fourier transform to spread continuously over the sampled area even though it is composed of discreet frequency components. Thus, the discreet frequency components must overlap forming a continuous distribution. Fortunately, this spreading occurs because the input aperture is finite.

By oversampling the Fourier components, we can modulate (or shift) the aperture function. To do this, we use bipolar modulation to change the sign of the pixels that straddle the ordinate of the Fourier components being sampled. As shown in Figure 3, this changes the phase profile of the envelope function shifted out by the discreet frequency components. To implement the phasor diagram shown in Figure 2, we need the pixels to be phase shifted by $\pi/2$ from each other or $\pm\pi/4$ from the ordinate of the frequency component. However, the bipolar modulator produces either a zero or π phase shift between the pixels which means we need to add or subtract a $\pi/2$ shift. This occurs through the spatial shift of the aperture function where it is shifted by zero or $\pm N/2$ (i.e. $\omega_o x_o = \pi$ where $\omega_o = 2\pi/N$). Assuming the aperture is a simple array of N elements and disregarding the effects of pixel width, the Fourier transform equation for the shifted aperture can be written as:

$$(e^{j\delta N}-1)/(e^{j\delta}-1),\ \text{or}\ \ e^{j(N-1)\delta/2}[\frac{\sin N\delta/2}{\sin\delta/2}], \tag{10}$$

where $\delta = \Delta 2\pi/N = \Delta\omega_o$ is the incremental phase shift per element.

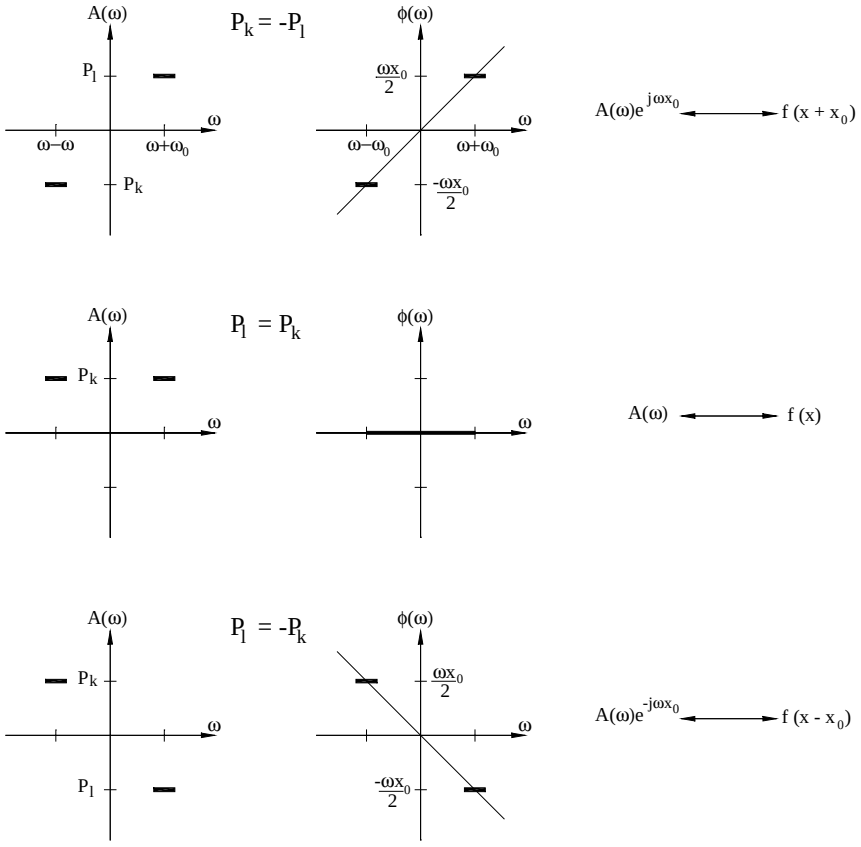

Figure 3. The effect of pixel modulation on the oversampled Fourier-domain components.

The sine-over-sine term in Equation 10 is a sinc function that envelopes the diffractive orders produced by the array factor. The amplitude part of the function goes to zero at $\pm 2\pi/N$ while the phase approaches $\pm\pi$. As discussed above, we need the phase shift at the pixels to be $\pm\pi/4$ which occurs when the pixels are spaced π apart in the frequency plane as shown in Figure 4 (i.e. $\pm(N-1)\delta/2=\pm\pi/4$ or $\pm N\delta=\pm\pi/2$).

If the modulated aperture function is not shifted ($p_k=p_l$), then the aperture remains an even function ($x_o=0$) and there is no phase shift at the pixels. Fortunately, the Fourier transform of an even-real function is an even-real function. The multiplication of these terms with a real number (real-axis modulation) produces real terms. It is only for the case where $p_k=-p_l$ that the aperture becomes an odd function ($x_o= \pm N/2$). Therefore, the phasor diagram of Figure 2 is not directly a result of the pixel's physical location. However, it is known from Fourier analysis that the following properties exist:

- Multiplying an **odd** and **even** function produces an **odd** function,
- Multiplying an **even** and **even** function produces an **even** function,
- Multiplying an **odd** and **odd** function produces an **even** function,

- Transforming an **odd-real** function produces an **odd-imaginary** function,
- Transforming an **even-real** function produces and **even-real** function.

With these properties and by shifting or not shifting the aperture of the even and odd terms of the function, the phasor diagram of Figure 2 is implemented in a round about way.

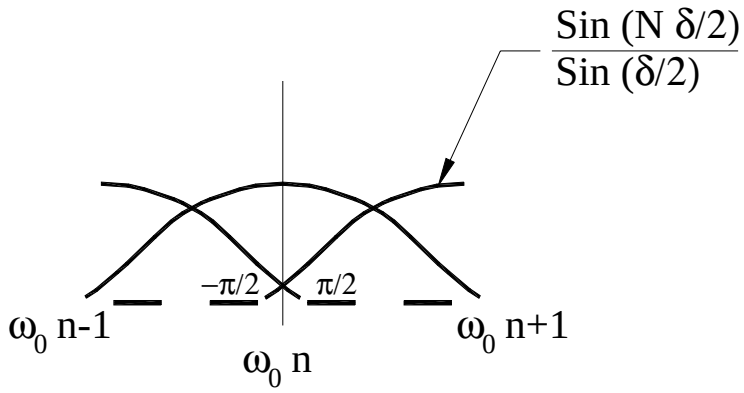

Figure 4. Pixel placement for sampling technique.

3. OPTICAL CONFIGURATION

In a frequency-plane correlator that uses pixelated transducers, it has been shown that the focal length between input and filter (or filter and detector) properly scales the sample spacing such that the Nyquist rate is achieved,[12] if

$$d_2 = \lambda f \,/\, N_1 d_1 \,, \tag{11}$$

where d_2 is the pixel spacing in the sample plane, λ is the wavelength of the carrier, f is the focal length of the transform lens, and $N_1 d_1$ is the sequence length of the input. Equation 11 actually indicates that the radius of the diffracted spot in the sample plane is a pixel width. If we place a pixel at the ordinate of $\omega_o(n)$, then the two adjacent pixels reside at $\omega_o(n+1)$ and $\omega_o(n-1)$. The technique presented in the preceding section requires that we increase the sample rate by a factor of two. By multiplying both sides of Equation 11 by two, we increase the sample rate either by doubling the carrier wavelength or focal length of the transform lens, or by halving the length of the input sequence. The best method is to change the focal length of the transform lens, since it is the easiest to physically implement without reducing the processing capacity of the optical system. The larger focal length spreads the Fourier transform over twice the area. This means that four times as many pixels are needed in the filter plane to fully sample the signal. Since SLM pixel density is not limitless, the increase in pixel count is definitely a disadvantage. Of course, there is no increase in pixel count if one is willing to give up resolution (i.e. the ability to distinguish the on to off transition of two adjacent pixels). For binary data applications such as analyzing pseudorandom digital codes, the reduction in resolution is not an option. For analog imagery, the loss of resolution is less of a concern.

As shown in Figure 4, the envelope of one frequency component falls to zero at the ordinate of the adjacent component. This overlap between frequency components (cross talk) is eliminated if we only sample at the ordinate locations. To fully eliminate crosstalk, the modulator also needs a zero-width pixel, which causes an efficiency problem. In practice, it is necessary for the pixel to have a non-zero fill factor, but maximizing fill factor increases crosstalk regardless of sampling technique. In our case, ordinate sampling is not possible. Therefore, the oversampling technique is prone to cross talk. To minimize this problem,

the pixel fill factor needs to be minimized. With today's backplanes, CCD arrays, and diode lasers, efficiency is not a major concern. A reduction of the pixel's fill factor to 50% or less is a feasible solution.

A final consideration is the method for reconstructing the sampled signal at the detector plane. If we oversample the signal in the filter plane generating a phase shift, then we cause these components to be diffracted to the first order causing them to translate about the zero-order. To reconstruct the correlation-plane image, we need to under-resolve the filter plane. This is accomplished by low-pass filtering the image (i.e. detecting only the central quarter of the correlation plane). Of course, this is implemented using the same technique discussed above for spreading out the Fourier spectrum in the filter plane. Therefore, we need, in both cases, the focal length of the transform lens to be increased so that the filter or correlation plane data is four times larger than the sample area. This is accomplished using the following formula

$$f_{1,2} = 2N_s d_s d_o / \lambda, \tag{12}$$

where f_1 and f_2 are the focal lengths of the lenses ($L_1$and L_2) shown in Figure 5, $N_s d_s$ represents the width of the filter SLM or CCD array, and d_o is the pixel pitch of the input or filter SLMs. If Equation 12 is divided by two, the scaling for Nyquist sampling is achieved.[13]

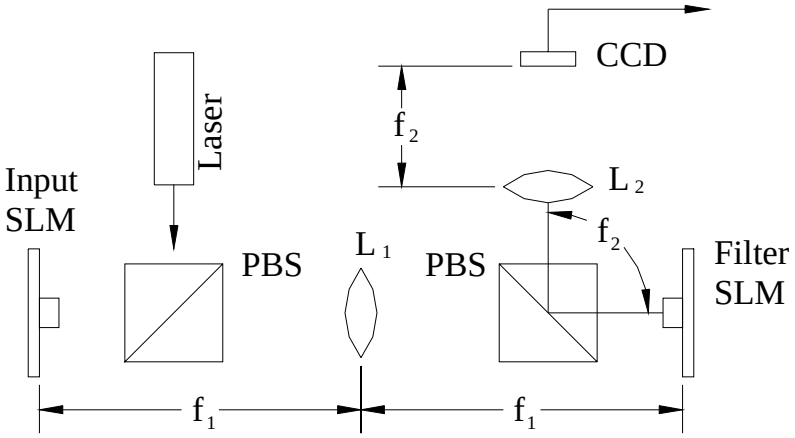

Figure 5. On-axis 4f-correlator configuration using reflective real-axis SLMs.

4. CONCLUSIONS

At the time of this paper's submission, the technique presented above has not been demonstrated in the lab. However, simulations using an FFT program verify that oversampling the data using a bipolar modulator produces the transform relationships described above. These simulations do not insure that the technique works since a complete front-to-back simulation of the method has not been completed.

If the technique works, it offers the following advantages:

- full complex modulation (independent control of amplitude and phase),
- on-axis (zero-order) operation,
- high-speed implementation (> 1000 fps using FLC modulator),
- high-resolution implementation (VLSI backplane compatible).

REFERENCES

1) Zeile, C. and E. Luder, "Complex transmission of liquid crystal spatial light modulators in optical signal processing applications," SPIE Vol. **1911**, pp. 195-206 (1993).
2) Brown, B. R. and A. W. Lohmann, "Complex spatial filtering with binary masks," Appl. Opt. **5**, pp. 967-969 (1966).
3) Lee, W. H., "Sampled Fourier transform hologram generated by computer," Appl. Opt. **9**, 639-643 (1970).
4) Burkhardt, C. B., "A simplification of Lee's method of generating holograms by computer," Appl. Opt. **9**, 1949 (1970).
5) Florence, J. M. and R. D. Juday, "Full-complex spatial filtering with a phase mostly DMD," in Wave Propagation and Scattering in Varied Media II, V. K. Varadan, ed., Proc. SPIE **1558**, 487-498 (1991).
6) Mendlovic, D. *et. al.*, "Encoding technique for design of zero-order (on-axis) Fraunhofer computer-generated holograms," Appl. Opt. **36**, 8427-8434 (1997).
7) Cohn, R. W., "Analyzing the Encoding Range of Amplitude-Phase Coupled Spatial Light Modulators," SPIE Vol. **3292**, 122-128 (1998).
8) Juday, R. D. and J. M. Florence, "Full complex modulation with two one-parameter SLMs," Proc. SPIE **1558**, 499-504 (1991).
9) Serati, S. A. and K. A. Bauchert, "Analog spatial light modulators: advances and applications," SPIE Vol. **3292**, 2-12 (1998).
10) Chao, T. H. and J. Yu, "Real-time Optical Correlator Using Computer-generated Holographic Filter on a Liquid Crystal Light Valve," SPIE Vol. **1347**, 211-220 (1990).
11) Kelly T. L. and J. Munch, "Improved kinoforms on spatial light modulators with less than π phase modulation capability," Opt. Eng. **37**, 1608-1611 (1998).
12) Bock, B. D., T. A. Crow and M. K. Giles, "Design considerations for miniature optical correlation systems that use pixelated input and filter transducers," SPIE Vol. **1347**, 297-309 (1990).
13) Davis, J. A., M. A. Waring, G. W. Bach, R. A. Lilly and D. M. Cottrell, "Compact optical correlator design," Appl. Opt. **28**, 10-11 (1989).